Max-Planck-Institut
für Mathematik
in den Naturwissenschaften
Leipzig

Spectral properties and synchronization in coupled map lattices

by

J. Jost and M. P. Joy

Preprint no.: 65 2001

Spectral Properties and Synchronization in Coupled Map Lattices

J. Jost[1,2] * and M. P. Joy[1] †
[1]Max Planck Institute for Mathematics in the Sciences
Inselstrasse 22-26, D-04103 Leipzig, Germany
[2] Santa Fe Institute, 1399 Hyde Park Road, Santa Fe, NM 87501, USA

September 25, 2001

Abstract

Spectral properties of Coupled Map Lattices are described. Conditions for the stability of spatially homogeneous chaotic solutions are derived using linear stability analysis. Global stability analysis results are also presented. The analytical results are supplemented with numerical examples. The quadratic map is used for the site dynamics with different coupling schemes such as global coupling, nearest neighbour coupling, intermediate range coupling, random coupling, small world coupling and scale free coupling.

PACS Numbers: 05.45.Ra, 05.45.Xt, 89.75.Hc

*email: jjost@mis.mpg.de
†email: mjoy@mis.mpg.de

1 Introduction

Synchronization of large interacting systems has been observed in several natural situations such as synchronized flashing of the fire flies, pace maker cells of the heart, neurons, etc [1, 2, 3]. Synchronization of chaos in low dimensional systems was studied by Pecora and Carroll [4]. It has also been studied in coupled oscillator systems and other spatially extended systems [5, 6]. Due to potential applications in various problems of practical interest, synchronization of chaotic elements in a coupled dynamical system has been an active area of research [7, 8].

Spatially extended systems are suitably modelled by coupled map lattices (CML). In comparison to partial differential equations, CMLs are more suitable for computational studies because of the discrete nature of time and space while all the analytical aspects of dynamical systems theory can also be used. CMLs were introduced as a simple model for spatio-temporal chaos [9]. They show a variety of phenomena from regular periodic behaviour to very complicated spatio-temporal patterns, chaos, intermittency, etc [10]. In CMLs, the dynamical elements are situated at discrete points in space, time is discrete, and the state variable is continuous. Each spatial unit is coupled to its neighbours. The selection of neighbours is determined by the structure of the network. In most studies diffusive coupling (nearest neighbour interaction) is used. There are studies on CMLs with various coupling schemes, such as open network, random network, global coupling , etc [11]. In most studies a symmetric coupling matrix is employed.

Here we study the synchronization properties of systems formed by a large number of identical dynamical elements that are connected by identical symmetrical links. We derive general conditions for the stability of spatially homogeneous solutions of a CML with any symmetric interaction matrix making use of the spectral properties of the interaction matrix. The coupling topology can affect crucially the synchronizability of the system.

In the next section we describe the properties of the spectrum of the CML. We perform a linear stability analysis and give the conditions for the stability of synchronous solutions and different regimes of stability. This is given in section 3. Results on the global stability analysis are given in section 4. In section 5 we provide some numerical results to elucidate the analytical results with specific examples. Here we take a quadratic map for the site dynamics as an example but the results are valid for any dynamical system. The results are even more general in the sense that their validity is not restricted just to CMLs, but can further be applied almost directly to partial differential equations, coupled ordinary differential equations, etc. Finally we provide a discussion on related aspects of the dynamics of CMLs.

2 CML and its Spectrum

We consider a coupled map lattice of the form,

$$u(x,n+1) = \epsilon \left(\frac{1}{n_x} \sum_{\substack{y \\ x \sim y}} f(u(y,n)) - f(u(x,n)) \right) + f(u(x,n)), \tag{1}$$

where n_x denotes the number of neighbours of x. Here, $f : R \to R$ is some differentiable function, often chosen to be the quadratic (logistic) map in the literature. x is a spatial variable, its domain being some finite discrete set M. That set carries a neighbourhood relationship, specifying which $y \in M$ are neighbours of a given x (notation: $x \sim y$). The extreme case is the one of a global coupling where all y are neighbours of any x. If M has the structure of a k-dimensional periodic grid, the other extreme case is the one of nearest neighbour coupling where only those y are neighbours of x that are one step away from x in one of the coordinate directions. In that case, each x has $2k$ neighbours. Of course, we also have the trivial case where each x is its own neighbour, but has no other neighbours. That case of course, represents the absence of coupling.

In the sequel, the only assumption we shall need is that the neighbourhood relationship is symmetric, i.e., if y is a neighbour of x, then x in turn is a neighbour of y. We also adopt the - completely inessential - convention that x is not considered as a neighbour of itself. (Abandoning that convention would simply amount to a redefinition of the value of ϵ.) Finally in order to avoid trivial case distinctions, we assume that the neighbourhood relationship is connected in the sense that for any given $x_1, x_2 \in M$, we find $y_1 = x_1, y_2, \ldots, y_m = x_2$, s.t. y_{j+1} is a neighbour of y_j for $j = 1, 2, \ldots, m-1$. We consider $n = 0, 1, 2, \ldots$, as the time variable of the evolution.

Our subsequent analysis will not depend in conceptual terms on the detailed structure of M. Of course, the numerical values of the bifurcation parameters below will reflect the geometry of M.

Our analysis is phrased in general terms and so it is straightforward to extend it to the cases:

- where f is vector valued,

- where M is a continuous space which then has to carry a measure $d\mu$, and the averaged sum needs to be replaced by an averaged integral,

- to weighted neighbourhoods i.e., where we are given a nonnegative function

$$h : M \times M \to R^+$$

that is symmetric ($h(x,y) = h(y,x) \quad \forall\ x, y \in M$) and consider in place of the averaged sum in equation (1)

$$(1/\sum_y h(x,y)) \sum_y h(x,y) f(u(y,n)),$$

(the situation in (1) corresponds to the choice $h(x,y) = \begin{cases} 1 & \text{if } x, y \text{ neighbours;} \\ 0 & \text{else} \end{cases}$),

- replacing the last term $f(u(x,n))$ in (1) by $g(u(x,n))$ for some function g,

- as well as to the case of coupled ordinary differential equations in place of difference equations.

As these extensions are rather trivial, we refrain from carrying them out.

The following represents a generalization of the linear stability analysis that has been carried out in the literature for various special cases such as global coupling [12], nearest neighbor coupling [13], and random coupling [14].

We shall need the L^2-product for functions on M:

$$(u,v) := \frac{1}{|M|}\sum_{x\in M} n_x u(x)v(x),$$

where $|M|$ stands for the number of elements of M. We also put $||u|| := (u,u)^{1/2}$, (L^2-norm of u). We consider the operator,

$$\mathcal{L} : L^2(M) \to L^2(M).$$

$$\mathcal{L}v(x) := \frac{1}{n_x}\sum_{\substack{y\\ x\sim y}} v(y) - v(x). \tag{2}$$

$\mathcal{L}$ has the following properties:

(i) $\mathcal{L}$ is selfadjoint w.r.t (.,.):

$$(u, \mathcal{L}v) = (\mathcal{L}u, v)$$

for all $u, v \in L^2(M)$. This follows from the symmetry of the neighbourhood relation.

(ii) $\mathcal{L}$ is nonpositive:

$$(\mathcal{L}v, v) \leq 0.$$

This follows from the Cauchy-Schwarz inequality.

(iii)

$$\mathcal{L}v = 0 \Longleftrightarrow v \equiv \text{constant}.$$

Hence, (i) implies that the eigenvalues of $\mathcal{L}$ are real. By (ii), they are nonpositive; we write them as $-\lambda_k$, and the eigenvalue equation then is

$$\mathcal{L}u_k + \lambda_k u_k = 0.$$

We order the eigenvalues as $\lambda_0 \leq \lambda_1 \leq \lambda_2 \leq \cdots \leq \lambda_K$. (This convention deviates from the one used in the literature. Our operator $\mathcal{L}$ corresponds to the interaction matrix minus the identity matrix, and one usually considers the eigenvalues of the former in descending order.)

We may then find an orthonormal basis of $L^2(M)$,

$$(u_k)_{k=1,\ldots,K}$$

of eigenvectors of $\mathcal{L}$.

By (iii) the smallest among the λ_k is

$$\lambda_0 = 0,$$

and this is a simple eigenvalue (because we assume that the neighbourhood relationship is connected), i.e.,

$$\lambda_k > 0 \text{ for } k > 0. \tag{3}$$

The numerical values of the bifurcation parameters occurring below will depend only (besides on ϵ and the Lyapunov exponent of f) on the eigenvalue spectrum of $\mathcal{L}$. This eigenvalue spectrum, of course, reflects the underlying geometry of M and of the coupling. Some general considerations may be helpful for understanding this point.

In the case of global coupling (including self coupling), we have

$$\lambda_0 = 0 \text{ (as always)}$$

and

$$\lambda_1 = \lambda_2 = \cdots = \lambda_k = 1,$$

since

$$\mathcal{L}v = -v$$

for any v that is orthogonal to the constant map, i.e., satisfies

$$\frac{1}{|M|}\sum_{y\in M} v(y) = 0.$$

If we shrink the neighbourhood size, then the eigenvalues can separate and grow, and in particular, the largest one, λ_K, will become larger the smaller the neighbourhood size is. In particular,

$$\lambda_K > 1$$

as there may exist $v \in L^2(M)$ with

$$\sum_{x\in M}\sum_{\substack{y\\ x\sim y}} v(x)v(y) < 0$$

(e.g. $M = \{1, 2, \ldots, m\}, m$ even, $m > 2$, with μ having neighbours $\mu - 1$ and $\mu + 1$, closed periodically, i.e. $m + 1 \equiv 1$,

$$v(\mu) = \begin{cases} 1, & \mu \text{ even}, \\ -1, & \mu \text{ odd} \end{cases}.$$

Conversely, if the neighbourhood interaction matrix of all points is the same and kept fixed while we increase the size of M, then all eigenvalues will decrease. This is a version of Courant's monotonicity theorem [15]. Thus, from our analysis below, synchronization will require, if possible at all, a larger value of the coupling parameter ϵ.

We also have the following version of Courant's nodal domain theorem [16]:

Lemma 1. *Consider M as a graph Γ_M, with an edge between x and y precisely if x and y are neighbours. Let u_k be an eigenfunction for the eigenvalue λ_k, with our above ordering, $0 = \lambda_0 < \lambda_1 \leq \lambda_2 \leq \cdots \leq \lambda_K$. Delete from the graph Γ_M all edges that connect points on which the values of u_k have opposite signs. This divides Γ_M into connected components $\Gamma_1, \ldots, \Gamma_l$. Then $l \leq k + 1$.*

3 Linear Stability Analysis

We now consider a solution $\bar{u}(n)$ of the uncoupled equation,

$$\bar{u}(n+1) = f(\bar{u}(n)). \tag{4}$$

Clearly, $u(x,n) = \bar{u}(n)$ then is a solution of (1). This solution is spatially homogeneous, or as one says, synchronized. The synchronization question then is whether for certain values of the coupling parameter ϵ, any solution of (1) asymptotically approaches a synchronized one. A somewhat weaker question is whether, when we consider a perturbation

$$u(x,n) = \bar{u}(n) + \delta\alpha_k(n)u_k(x), \tag{5}$$

by an eigenmode u_k for some $k \geq 1$, and small enough δ, $\alpha_k(n)$ goes to 0 for $n \to \infty$, if $u(x,n)$ solves (1). That question can be investigated by linear stability analysis and we proceed to carry that out. Inserting (5) into (1) and expanding about $\delta = 0$ yields

$$\alpha_k(n+1) = (1 - \epsilon\lambda_k)f'(\bar{u}(n))\alpha_k(n), \tag{6}$$

f' denoting the derivative of f. So the sufficient local stability condition

$$\lim_{N\to\infty} \frac{1}{N} \log \frac{\alpha_k(N)}{\alpha_k(0)} = \lim_{N\to\infty} \frac{1}{N} \log \prod_{n=0}^{N-1} \frac{\alpha_k(n+1)}{\alpha_k(n)} < 0 \tag{7}$$

becomes

$$\log|1 - \epsilon\lambda_k| + \lim_{N\to\infty} \frac{1}{N} \sum_{n=0}^{N-1} \log|f'(\bar{u}(n))| < 0. \tag{8}$$

Here,

$$\mu_0 = \lim_{N\to\infty} \frac{1}{N} \sum_{n=0}^{N-1} \log|f'(\bar{u}(n))|$$

is the Lyapunov exponent of f and so the stability condition (8) is

$$|e^{\mu_o}(1 - \epsilon\lambda_K)| < 1. \tag{9}$$

We may have

$$\mu_o > 0, \tag{10}$$

i.e. temporal instability, but (9) for all $k \geq 1$; i.e. synchronization. We shall now assume (10) for the remainder of this section. By our ordering convention for the eigenvalues, (9) holds for all $k \geq 1$ if

$$\frac{1 - e^{-\mu_o}}{\lambda_1} < \epsilon < \frac{1 + e^{-\mu_o}}{\lambda_K}. \tag{11}$$

In order to satisfy that condition, we need

$$\frac{\lambda_K}{\lambda_1} < \frac{e^{\mu_o}+1}{e^{\mu_o}-1}. \tag{12}$$

By our above discussion this hold in the globally coupled case because there $\lambda_K = \lambda_1$. By way of contrast if we have nearest neighbour coupling, this can only hold if the size of M is not too large. (For a 1-dimensional chain, the critical size is 5, with a large value of ϵ. If we have second nearest neighbour coupling, the critical size of a one dimensional chain is 9.)

Let us now assume that (12) holds. We then predict the following behaviour of the coupled system as ϵ increases.

For very small values of $\epsilon > 0$, as we assume (10)

$$e^{\mu_o}(1-\epsilon\lambda_k) > 1,$$

and so, all spatial modes $u_k, k \geq 1$, are unstable, and no synchronization occurs. If we are in the globally coupled case, then there exists a single critical value ϵ_c such that

$$e^{\mu_o}(1-\epsilon_c\lambda_k) = 1$$

for all $k = 1, 2, \ldots, K$. For $\epsilon > \epsilon_c$, the dynamics become synchronized. For ϵ slightly smaller than ϵ_c, one observes intermittent behaviour, clustering, etc [17].

Let us now consider the more interesting case where the coupling is not global so that not all the λ_k are equal; in particular

$$\lambda_1 < \lambda_K.$$

We then let ϵ_k be the solution of

$$e^{\mu_o}(1-\epsilon_k\lambda_k) = 1$$

The smallest among these values is ϵ_K, the largest ϵ_1. If now, for $k_1 < k_2$,

$$\epsilon_{k_2} < \epsilon < \epsilon_{k_1}$$

then the modes $u_{k_2}, u_{k_2+1}, \ldots, u_K$ are stable, while the modes $u_1, u_2, \ldots, u_{k_1}$ are unstable. Because of Lemma 1, we see that desynchronization can lead to utmost k_2+1 subdomains on which the dynamics is either advanced or retarded.

In particular, if ϵ increases, first the highest modes, i.e., the ones with most spatial oscillations, become stabilized, and the mode u_1 becomes stabilized the last. So if $\epsilon_2 < \epsilon < \epsilon_1$, then any desynchronized state consists of two subdomains.

We then let $\bar{\epsilon_k}$ be the solution of

$$e^{\mu_o}(\bar{\epsilon_k}\lambda_k - 1) = 1$$

Again,

$$\bar{\epsilon_k} \leq \bar{\epsilon}_{k-1}.$$

Because of (11),

$$\epsilon_1 < \bar{\epsilon}_K .$$

If

$$\epsilon_1 < \epsilon < \bar{\epsilon}_K ,$$

then all modes $u_k, k = 1, 2, \ldots , K$, are stable, and the dynamics synchronizes.

If ϵ increases beyond $\bar{\epsilon}_K$, then the highest frequency mode u_K becomes unstable and we predict spatial oscillations of high frequency of a solution of the dynamics . If ϵ increases further then more and more spatial modes become destabilized.

4 Global Stability Analysis

The basis of the preceding analysis was a linear expansion about a synchronized state $\bar{u}(n)$. Therefore, that analysis is valid only for small perturbations about such a state. In this section, we want to derive a criterion that guarantees synchronization for arbitrary starting values $u(x, 0)$ of a solution of (1).

From general principles of functional analysis (see [18]), there exists an operator,

$$\Lambda : L^2(M) \to L^2(M)$$

with

$$-(u, \mathcal{L}v) = (\Lambda u, \Lambda v), \forall u, v \in L^2(M). \tag{13}$$

This follows from the self adjointness of $\mathcal{L}$. It is not difficult to write a Λ down explicitly, but our more abstract approach provides the advantage of a less cumbersome notation.

Λ is nonnegative in the sense that

$$(\Lambda u, \Lambda u) \geq 0, \forall u \in L^2(M), \tag{14}$$

and we even have

$$\Lambda u = 0 \Longleftrightarrow u \equiv \text{constant} \tag{15}$$

(This follows from the nonpositivity properties of $\mathcal{L}$).

Moreover Λ commutes with $\mathcal{L}$, i.e.,

$$\Lambda\mathcal{L} = \mathcal{L}\Lambda, \tag{16}$$

and so, we may assume that the u_k are also eigenfunctions of Λ.

Therefore a natural ansatz for a Lyapunov function for the dynamics (1) is

$$\Phi(n) := (\Lambda u(., n), \Lambda u(., n)), \tag{17}$$

and it remains to derive conditions under which

$$\Phi(n) \to 0, \text{for } \ n \to \infty. \tag{18}$$

We have

$$\begin{aligned}\Phi(n+1) &= (\Lambda u(.,n+1), \Lambda u(.,n+1)) \\ &= (\Lambda u(.,n+1), \Lambda(\epsilon L f(.,n) + (1-\epsilon) f(.,n)))\end{aligned}$$

by (1).

Since the u_k are an orthogonal basis of $L^2(M)$, we may write

$$f(u(x,n)) = \sum_{k=0}^{K} \beta_k(n) u_k(x),$$

with $\beta_k(n) = (f(u(.,n)), u_k)$. Inserting this into the last equality, we get

$$\Phi(n+1) = \left(\Lambda u(.,n+1), \Lambda \sum_{k=0}^{K} (1-\epsilon\lambda_k)\beta_k(n) u_k \right). \tag{19}$$

The important observation now is that in the last sum, we can discard the summand $k=0$, because u_0 is constant, and so

$$\Lambda u_0 = 0.$$

Moreover, we observed above that, since Λ commutes with $\mathcal{L}$, we may assume,

$$(\Lambda u_k, \Lambda u_l) = 0, \text{for } \; k \neq l,$$

and so

$$||\Lambda f(u(.,n))||^2 = \sum_{k=0}^{K} \beta_k^2(n) ||\Lambda u_k||^2.$$

Using these observations and the Cauchy-Schwarz inequality in (18), we may estimate

$$\Phi(n+1) \leq \frac{1}{2}||\Lambda u(.,n+1)||^2 + \frac{1}{2}(1-\epsilon\lambda_1)^2 ||\Lambda f(u(.,n))||^2, \tag{20}$$

assuming $|1-\epsilon\lambda_K| \leq 1-\epsilon\lambda_1$, i.e.,

$$\epsilon \leq \frac{2}{\lambda_1 + \lambda_K}. \tag{21}$$

If we now use the coarse estimate

$$||\Lambda f(u(.,n))|| \leq \sup |f'| ||\Lambda u(.,n)||, \tag{22}$$

we obtain from (20)

$$\Phi(n+1) \leq (1-\epsilon\lambda_1)^2 \sup |f'|^2 \Phi(n). \tag{23}$$

We conclude

Theorem 1. *The coupled dynamical system (1) asymptotically synchronizes if ϵ satisfies (21) and*

$$(1 - \epsilon\lambda_1) \sup |f'| < 1. \tag{24}$$

Remark: If (21) does not hold, (24) needs to be replaced by,

$$(\epsilon\lambda_K - 1) \sup |f'| < 1. \tag{25}$$

In the special case of global coupling, the synchronization condition becomes,

$$(1 - \epsilon) \sup |f'| < 1, (0 \leq \epsilon < 1) \tag{26}$$

The reason why we have $\sup |f'|$ in (24), in place of e^{μ_0}, μ_0 being the Lyapunov exponent of f, as in section 3, is that here we do not linearize about a spatially homogeneous solution. Our global approach rather requires to consider any solution $u(x, n)$ of (1). This means, however, that our condition (11), while sufficient, need not be necessary for synchronization.

5 Numerical Results

In this section we demonstrate our results with different coupling schemes or network topology. For our numerical study we took the quadratic map for the site dynamics. The quadratic map is a widely studied chaotic map, given by $f(x) = 1 - ax^2$ [19]. Here a is a parameter and varying its value the single map shows a variety of dynamical phenomena. It becomes chaotic when $a \approx 1.4011$, going through a period doubling bifurcation sequence. At $a = 2$ the map is maximally chaotic, with a Lyapunov exponent $\mu_0 = \log(2)$.

5.1 Global coupling

In the case of global coupling, we have $\lambda_0 = 0$ and $\lambda_1 = \lambda_2 = \cdots = \lambda_{m-1} = 1$. (The self coupling term is also included here.) This case has been studied in various contexts. When $\exp(\mu_0)(1 - \epsilon) < 1$, the spatially homogeneous solution is stable, as shown in [12]. For the quadratic map with $a = 2$, it becomes stable when $\epsilon > 0.5$. Just below this value the system shows spatio temporal intermittency, clustering phenomena, etc [10]. In Fig. 1(a), we display $\sigma(n)$, the fluctuation of the state variable from the mean, defined by $\sigma^2(n) = \frac{1}{m}\sum_{i=1}^{m}(x_i(n) - \bar{x}(n))^2, (\bar{x}(n)$ is the average of all $x_i(n))$, for different values of ϵ, for the case with $a = 2.0$. It can be seen that when $\epsilon > \epsilon_c = 0.5$, the value of σ becomes zero (within the numerical accuracy) indicating that the system is synchronized. Though the linear stability does not guarantee the synchronization from arbitrary initial conditions, in this case it happens. We started with random initial conditions for the individual sites, and after a few iterations the system synchronizes, indicating the stability of the spatially homogeneous solutions in these parameter regimes. For $a = 1.9$, the system synchronizes for a smaller value of ϵ, since the Lyapunov exponent at that parameter value is 0.5490. Here the critical value is $\epsilon_c = 0.4225$. Figure 1(b) gives details of this case. We took $m = 1000$ for our simulations.

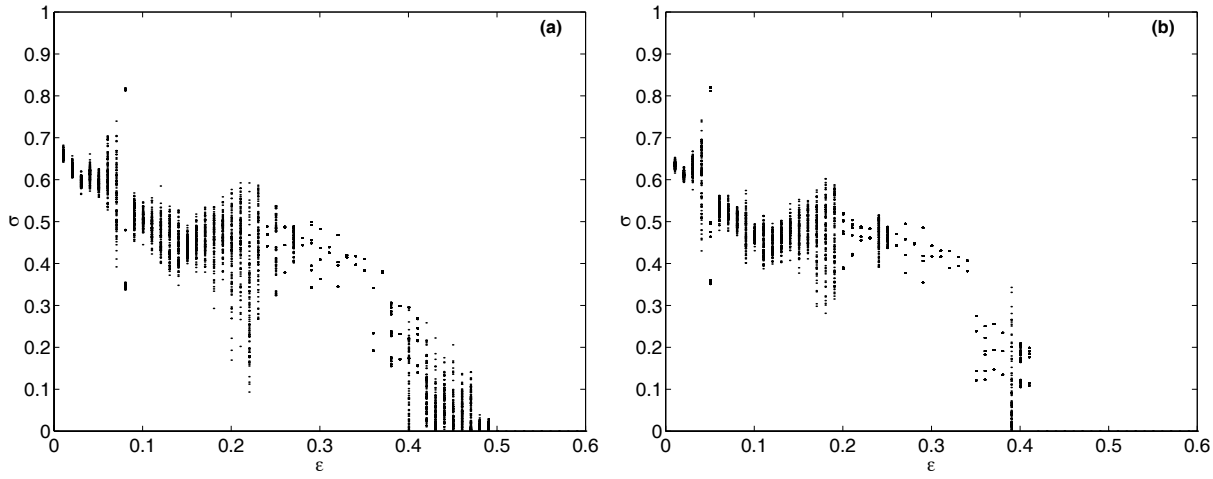

Figure 1: Fluctuation of the mean, $\sigma(n)$ is shown as a function of the coupling strength, ϵ. At each value of ϵ, 200 final iterates of $\sigma(n)$ are plotted. Here $m = 1000$ and the coupling is global. In (a) $a = 2.0$, and in (b) $a = 1.9$.

5.2 Nearest Neighbour Coupling

Here the eigenvalues are given by $\lambda_0 = 0$ and $\lambda_i = 1 - \cos(\frac{2\pi i}{m}), i = 1, 2, 3, \ldots, m-1$. The first nonzero eigenvalue is

$$\lambda_1 = 1 - \cos(\frac{2\pi i}{m}),$$

and the largest eigenvalue is

$$\lambda_K = \begin{cases} 2 & \text{for even } m \\ 1 + \cos(\frac{\pi}{m}) & \text{for odd } m \end{cases}.$$

Using this one can calculate the maximum value of m at which the spatially homogeneous solution can be stable using the condition for linear stability. It will occur when

$$\frac{\lambda_K}{\lambda_1} < \frac{\exp(\mu_0) + 1}{\exp(\mu_0) - 1}$$

and the value of ϵ lying between

$$\frac{1 - \exp(-\mu_0)}{\lambda_1} < \epsilon < \frac{1 + \exp(-\mu_0)}{\lambda_K}.$$

For a CML with a fully chaotic quadratic map the maximum value of the system size which can sustain a stable synchronous solution is $m = 5$, when ϵ is between 0.5 and 0.78. In the case of $m = 6$, the first mode becomes stable at $\epsilon = 1$, but the last mode becomes unstable for a value of ϵ above 0.75. Hence there is no synchronization. The second mode is stable when ϵ is between 0.333 and 1. In Figs. 2–3 we give the plot of the fluctuation of the mean field for different values of ϵ, for $m = 5$ and $m = 6$, when $a = 2.0$ (a) and $a = 1.9$ (b). When $m = 6$, between $\epsilon = 0.33$ and 0.75 only one mode is unstable. From

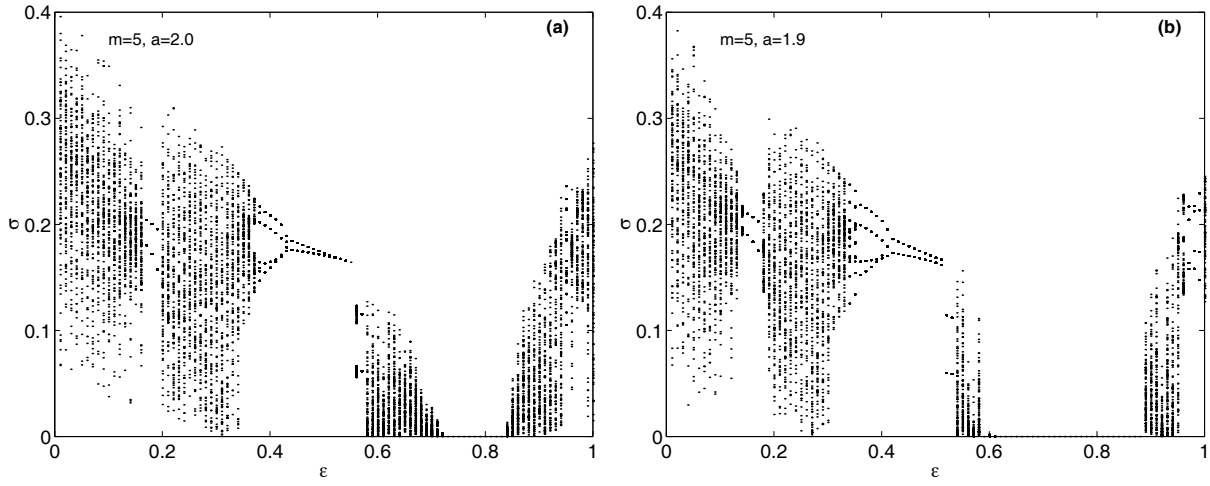

Figure 2: Same as in Fig. 1 with nearest neighbour coupling, for $m = 5$, in (a) $a = 2.0$, and in (b) $a = 1.9$.

the spectrum one can see that the largest value of m for which only the first mode is unstable is $m = 9$ when $0.72 < \epsilon < 0.75$. For higher values of m more than one mode will be unstable for any value of ϵ. So there cannot be synchronization in large systems with nearest neighbour coupling.

5.3 Intermediate Range Coupling

If we consider k nearest neighbours (there will be $2k$ neighbours for each site) the eigenvalues are given by $\lambda_0 = 0$ and

$$\lambda_i = 1 - \frac{1}{2k} \sum_{j=1}^{k} \cos(\frac{2\pi ij}{m}), i = 1, 2, \ldots, m-1.$$

Let us consider the case of two nearest neighbours ($k = 2$). As in the case of NN coupling one can find the maximum value of m at which the CML can sustain stable synchronous chaotic oscillations. For k=2, it is $m = 9$ with $0.33 < \epsilon < 1$. The maximum value of m at which the second largest mode also becomes unstable is $m = 18$. Figure 4 gives the plot for $m = 9$ for $a = 2.0$ (a) and $a = 1.9$ (b). For 3 nearest neighbours ($k = 3$), it is at $m = 12$, and for $k = 4, m = 15$.

One can see that for $k/m > 0.301$ the system synchronizes when the coupling is strong, i.e., $\epsilon = 1$. In Fig. 5 $\sigma(n)$ is shown as a function of k for $m = 1000$ near the synchronization transition region. In each grid corresponding to a k value, 1000 final iterates of $\sigma(n)$ are plotted after discarding initial transients. The system shows synchronization when $k = 301$. As the system size increases we need a higher number of neighbours for synchronization. For a fixed number of neighbours the behaviour is like that of the NN case; there is no synchronization when the system size increases.

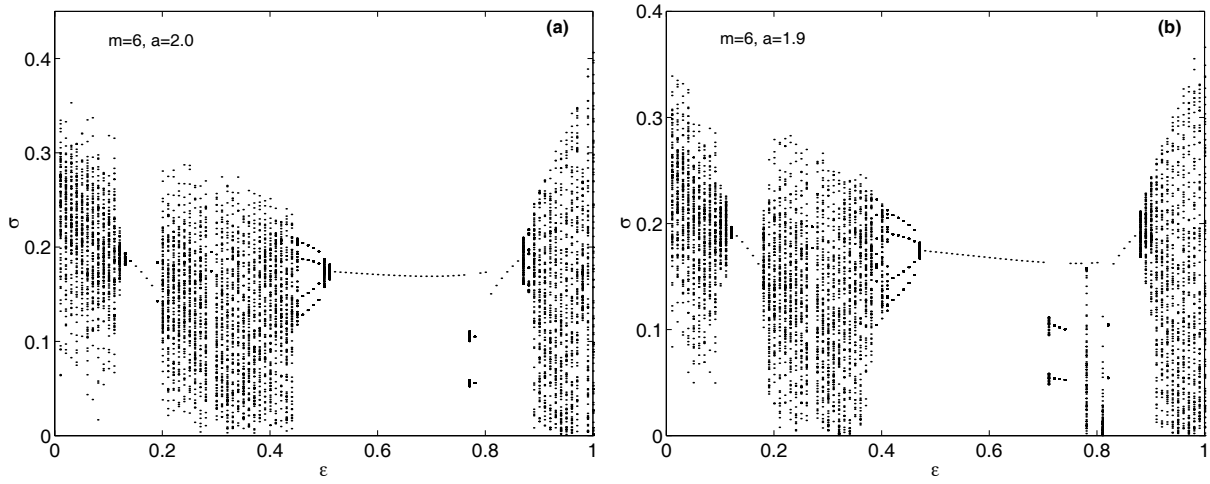

Figure 3: Same as in Fig. 2 with nearest neighbour coupling, for $m = 6$.

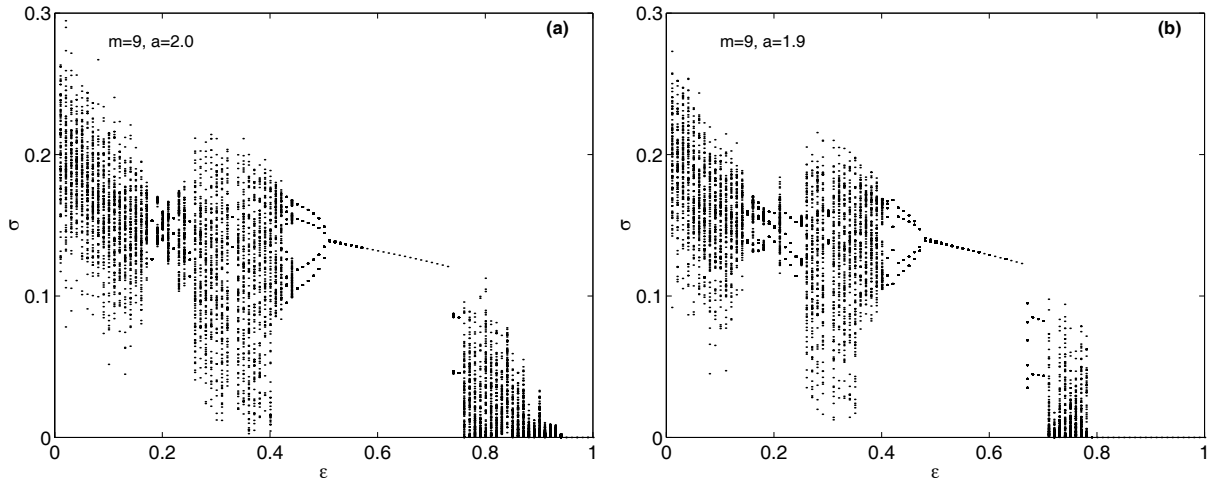

Figure 4: Same as in Fig. 2 with two nearest neighbours coupling, for $m = 9$.

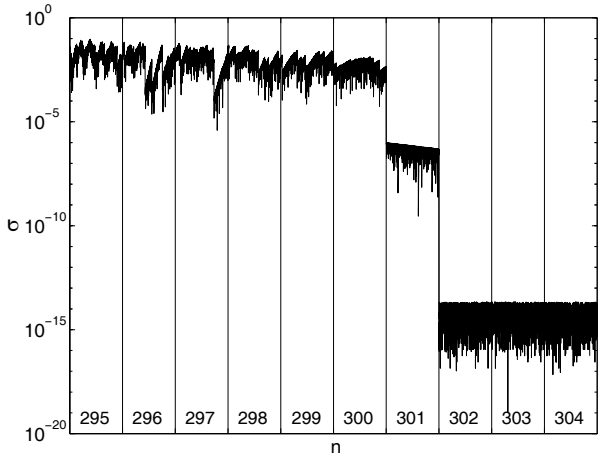

Figure 5: Here $\sigma(n)$ is plotted for different values of k (denoted inside the grid) with intermediate range coupling, for $m = 1000, a = 2.0$, and $\epsilon = 1.0$. Between two grid lines 1000 iterates of $\sigma(n)$ are plotted.

5.4 Random Coupling

Now we consider a case where there is coupling between random sites. For every site we randomly select k other distinct sites and connect them with each other under the constraint that self and multiple coupling is prohibited. The average degree of a node in such a graph obtained is $2k$. For the quadratic map with $a = 2.0$ and $\epsilon = 1$, the system synchronizes for large m, if $k > 8$, in contrast to the unsymmetric case where it does so for $k > 4$ [14].

We plot the fluctuation of the mean field, σ, for different values of k for $m = 1000$, $\epsilon = 1.0$, $a = 2.0$ (Fig. 6(a)), and $a = 1.9$ (Fig. 6(b)). It can be seen that the system synchronizes when the average degree of a vertex is 8 or more, for the completely chaotic quadratic map. This is independent of the system size m. From random matrix theory one can see that the value of λ_1 depends only on k [20]. For smaller m, synchronization can occur below $k = 8$ because of the finite system size effects. So unlike in the case of nearest neighbour or intermediate range interactions, in the case of random coupling, one can have chaotic synchronization for any arbitrarily large value of m, if the number of neighbours (k) is larger than some threshold determined by the value of the maximal Lyapunov exponent of the chaotic map.

5.5 Small-world Networks

Small-world (SW) networks have an intermediate connectivity between regular and random networks. They are characterized by a very small mean path length as in random networks while at the same time having a high clustering coefficient as in regular networks. SW coupling is done as in the Watts and Strogatz algorithm [21]. We start with a lattice of m vertices each connected to its k neighbours. With a probability p we reconnect each

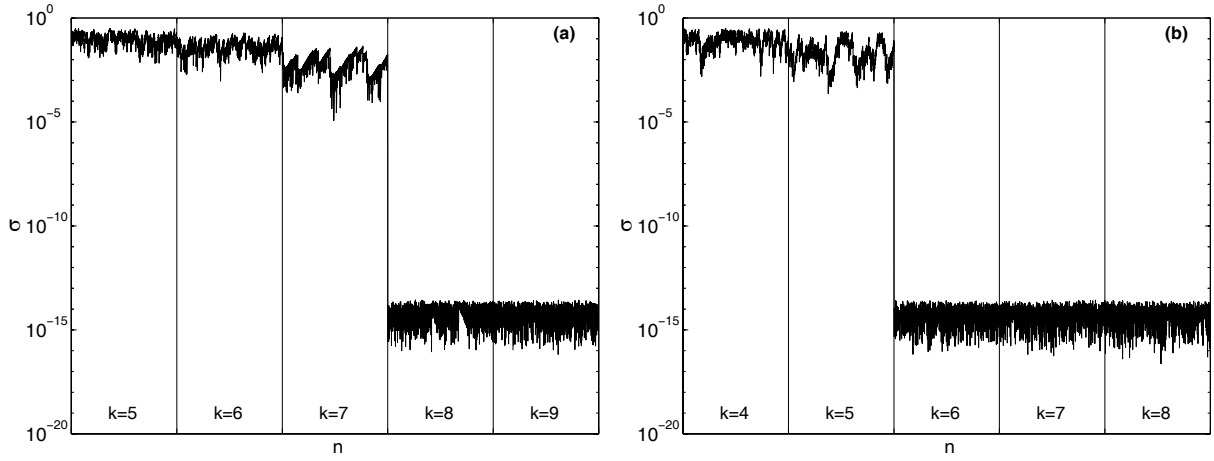

Figure 6: Same as in Fig. 5 with random coupling for different k values, for $m = 1000$, and $\epsilon = 1.0$. In (a) $a = 2.0$ and in b) $a = 1.9$.

edge to a vertex chosen uniformly at random over the entire lattice. Duplicate edges are avoided. It has been shown in [21] that even for a very small random rewiring probability p there is a transition to the small-world regime.

Here we took $p = 0.1$ at which there is small world effect on the structural properties of the graph. Figure 7 gives the fluctuation $\sigma(n)$ for different values of ϵ, $k = 10$ and $m = 1000$. One can see that there is no synchronization at this value of p, $\lambda_1 \approx 0.08$. When $p = 0.8$, there is synchronization for $\epsilon = 1.0$. At this value the number of random connections per vertex reaches the value needed for synchronization. In Fig. 8, $\sigma(n)$ is plotted for p values from 0.0001 to 1, and $\epsilon = 1.0$. Between two grid lines 1000 iterates of $\sigma(n)$ are plotted and the corresponding $\log_{10}(p)$ values are also denoted. From this figure we can easily see that there is no synchronization for smaller p values.

5.6 Scale-free Networks

Another widely studied class of networks are the scale free networks, where the degree distribution obeys a power law which is observed in many real networks. We studied the synchronization of a scale free network constructed by the Barabasi-Albert algorithm [22]. We start with k_0 vertices and at every time a new node is introduced. The new node is connected to k already existing nodes and they are selected with a probability proportional to the degree of that node. The process is continued for a long time and then the degree distribution is described by the power law, $P(k) \sim k^{-\gamma}$, where $\gamma = 3$. It is independent of k_0. For this study we took $k_0 = k$ and a network of size $m = 1000$. Figure 9 shows the σ versus ϵ plot for $k = 6$, and $a = 1.9$. In Fig. 10, $\sigma(n)$ is plotted for different values of k, for the case $a = 1.9$. The synchronization behaviour is comparable to that of a random network. When $k > 8$ there is synchronization for $a = 2.0$. We checked our results with higher values of m also. The results seem to converge for large system sizes and to be independent of the time of evolution (size) of the network.

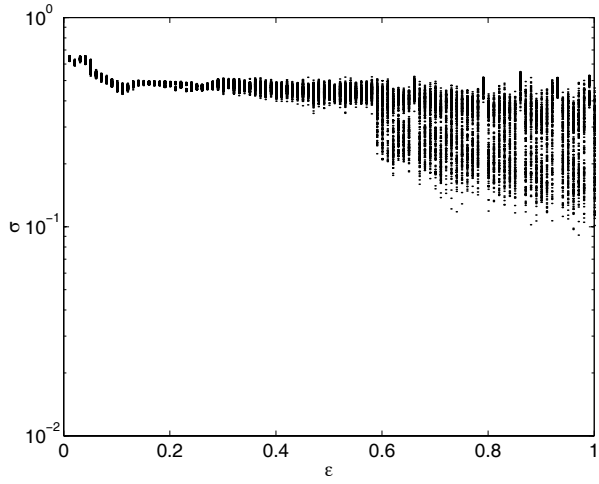

Figure 7: Same as in Fig. 1 with small-world coupling, for $m = 1000, k = 10$, $a = 2.0$, and $p = 0.1$.

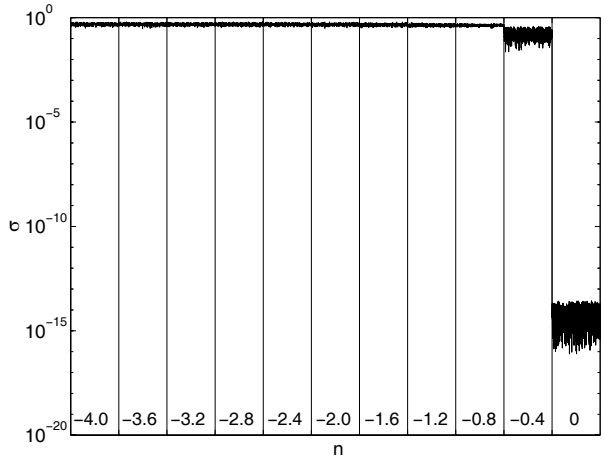

Figure 8: $\sigma(n)$ for different values of p with small-world coupling, for $m = 1000, k = 10$, $a = 2.0$ and $\epsilon = 1$. Between two grid lines, corresponding to a p value, 1000 iterates of $\sigma(n)$ are plotted and the corresponding $\log_{10}(p)$ is denoted at the bottom.

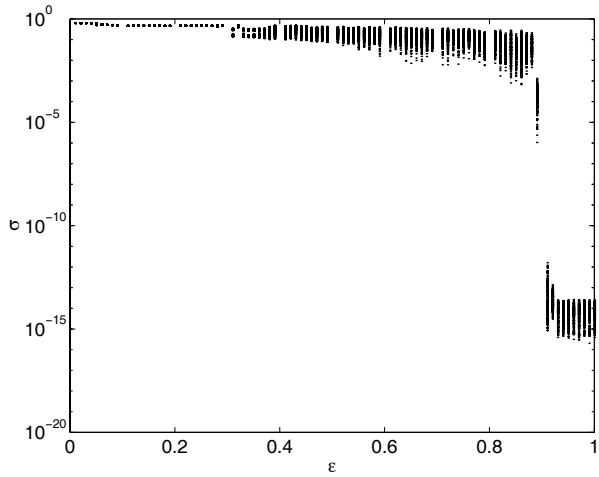

Figure 9: Same as in Fig. 1 with scale free coupling, for $m = 1000, k = 6$ and $a = 1.9$.

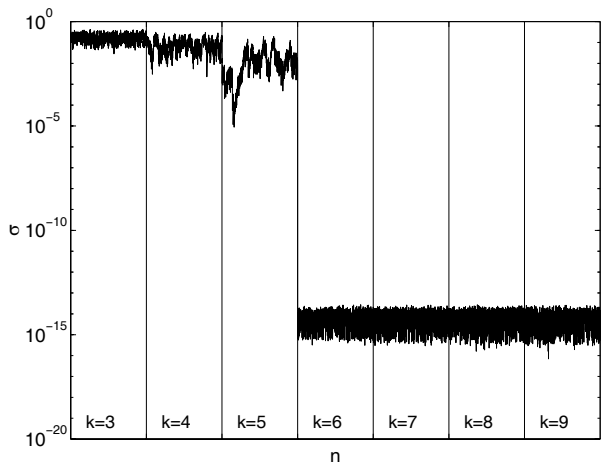

Figure 10: Same as in Fig. 5 with scale free coupling, for $m = 1000, a = 1.9$ and $\epsilon = 1.0$.

6 Conclusion

We studied the spectrum of coupled map lattices and its relation to the stability properties of the spatially homogeneous solutions. We derived conditions for the existence of such solutions using linear stability analysis. Conditions obtained from a global stability analysis are also provided. Our results are supplemented with numerical examples. For the numerical study the quadratic (logistic) map is used for the site dynamics. We studied the synchronization properties of coupled map lattices with different coupling topologies such as global coupling, nearest neighbour coupling, intermediate range coupling, random coupling, small-world coupling and real-world coupling. The coupling topology can crucially influence the synchronizability of the CML. Our study can be generalized almost directly to other spatially extended systems.

Acknowledgements

We thank Thomas Wennekers for the critical reading of the manusript.

References

[1] S. H. Strogatz and I. Stewart, Coupled oscillators and biological synchronization, *Sci. Am.*, 269(6):102–109, 1993.

[2] C. M. Gray, Synchronous oscillations in neuronal systems: Mechanisms and functions, *J. Comp. Neurosci.*, 1:11–38, 1994.

[3] L. Glass, Synchronization and rhythmic processes in physiology, *Nature*, 410:277–284, 2001.

[4] L. M. Pecora and T. L. Carroll, Synchronization in chaotic systems, *Phys. Rev. Lett.*, 64:821–824, 1990.

[5] R. E. Mirollo and S. H. Strogatz, Synchronization properties of pulse-coupled biological oscillators, *SIAM J. Appl. Math.*, 50:1645–1662, 1990.

[6] J. F. Heagy, T. L. Carroll, and L. M. Pecora, Synchronous chaos in coupled oscillator systems, *Phys. Rev. E*, 50:1874–1885, 1994.

[7] M. Lakshmanan and K. Murali, *Chaos in nonlinear oscillators: Controlling and Synchronization*, (World Scientific, Singapore, 1996).

[8] A. Pikovsky, M. Rosenblum, and J. Kurths, *Synchronization: A Universal Concept in Nonlinear Sciences*, (CUP, Cambridge, 2001).

[9] K. Kaneko, Period-doubling of kink-antikink patterns, quasi-periodicity in antiferro-like structures and spatial-intermittency in coupled map lattices - toward a prelude to a field theory of chaos, *Prog. Theor. Phys.*, 72:480–486, 1984.

[10] K. Kaneko and I. Tsuda, *Complex Systems: Chaos and Beyond*, (Springer, Berlin, 1996).

[11] K. Kaneko, (Ed.), *Theory and Applications of Coupled Map Lattices*, (Wiley, New York, 1993).

[12] K. Kaneko, Clustering, coding, switching, hierarchical ordering, and control in a network of chaotic elements, *Physica D*, 41:137-172, 1990.

[13] P. M. Gade and R. E. Amritkar, Spatially periodic orbits in coupled map lattices, *Phys. Rev. E*, 47:143-154, 1993.

[14] P. M. Gade, Synchronization of oscillators with random nonlocal connectivity, *Phys. Rev. E*, 54:64–70, 1996.

[15] R. Courant and D. Hilbert, *Methods of Mathematical Physics*, (Interscience, New York, 1943).

[16] E. B. Davies, J. Leydold, and P. F. Stadler, Discrete nodal domain theorems, arXiv:math.SP/0009120, 2000.

[17] K. Kaneko, Pattern dynamics in spatiotemporal chaos, *Physica D*, 34:1–41, 1989.

[18] K. Yosida, *Functional Analysis*, (Springer-Verlag, Berlin, 1980).

[19] P. Collet and I. P. Eckmann, *Iterated maps on the interval as dynamical systems*, (Birkhauser, Boston, 1980).

[20] B. Bollobas, *Random Graphs*, (Academic Press, London, 1985).

[21] D. J. Watts and S. H. Strogatz, Collective dynamics of 'small-world' networks, *Nature*, 393:440–442, 1998.

[22] A. L. Barabasi and R. A. Albert. Emergence of scaling in random networks, *Science*, 286:509–512, 1999.